Millimeter Wave WPAN: Cross-Layer Modeling and Multihop Architecture

Sumit Singh*, Federico Ziliotto†, Upamanyu Madhow*, Elizabeth M. Belding-Royer‡ and Mark J. W. Rodwell*
*Department of Electrical and Computer Engineering,
University of California, Santa Barbara
†Department of Information Engineering,
University of Padova, Padova, Italy
‡Department of Computer Science,
University of California, Santa Barbara

***Abstract*— The 7 GHz of unlicensed spectrum in the 60 GHz band offers the potential for multiGigabit indoor wireless personal area networking (WPAN). With recent advances in the speed of silicon (CMOS and SiGe) processes, low-cost transceiver realizations in this "millimeter (mm) wave" band are within reach. However, mm wave communication links are more fragile than those at lower frequencies (e.g., 2.4 or 5 GHz) because of larger propagation losses and reduced diffraction around obstacles. On the other hand, directional antennas that provide directivity gains and reduction in delay spread are far easier to implement at mm-scale wavelengths. In this paper, we present a cross-layer modeling methodology and a novel multihop medium access control (MAC) architecture for efficient utilization of 60 GHz spectrum, taking into account the preceding physical characteristics. We propose an in-room WPAN architecture in which every link is constrained to be directional, for improved power efficiency (due to directivity gains) and simplicity of implementation (due to reduced delay spread). Thus, obstacles that fall in the line of sight (LOS) path between transmitter and receiver result in link outage. We develop an elementary diffraction-based model to determine network link connectivity as a function of stationary and moving obstacle locations in the room. We define a multihop MAC protocol that accounts for directional transmission/reception, including procedures for topology discovery and recovery from link blockages. The proposed multihop MAC architecture is shown to be effective in maintaining network connectivity in scenarios where single hop communication suffers significant outages due to obstacles.**

I. Introduction

The 60 GHz band has been allocated worldwide for short range wireless communications because high atmospheric path loss due to oxygen absorption renders it unsuitable for long distance communications [1], [2]. The abundant unlicensed spectrum around 60 GHz (7 GHz in the US, with 3 GHz of unlicensed bandwidth common to the US, Europe and Japan) has the potential to enable numerous indoor wireless applications that require large bandwidth such as streaming content download (for High Definition Television (HDTV), video on demand, home theater, etc); high speed Internet access; real time streaming and wireless gigabit Ethernet for laptops and desktops [3]. These applications cannot be supported over existing home networking solutions (IEEE 802.11 a/b/g) because the required data rates (of the order of gigabits per second) far exceed their capabilities. As a result, 60 GHz communication is attracting significant interest from both industry and academia, leading to active research and standardization efforts for this technology [4], [5], [6]. The IEEE 802.15 WPAN Millimeter Wave Alternative PHY Task Group 3c formed in March 2005 is working towards standardizing the physical (PHY) layer for WPANs operating in the 60 GHz band [3].

To leverage the potential of 60 GHz communication, we present a cross-layer modeling methodology and a novel multihop MAC architecture for robust, multiGigabit, in-room WPANs using 60 GHz mm wave spectrum. In the following text, we outline some critical design considerations and describe the major components of our 60 GHz WPAN architecture.

Design Considerations: The successful harnessing of 60 GHz spectrum for multiGigabit indoor WPANs requires cross-layer design based on an understanding, at least at a coarse level, of the unique physical layer properties of mm wave communication. We enumerate some relevant design considerations below. It is useful to contrast 60 GHz communication with the more familiar 5 GHz microwave band used for unlicensed IEEE 802.11a WLANs in order to emphasize the need for a different approach to network design:

- Since free space propagation loss scales up as the square of the carrier frequency, the propagation loss for 60 GHz is more than 20 dB worse than that at 5 GHz.
- Directional antennas are far easier to implement at 60 GHz than at 5 GHz because of the smaller wavelengths. In particular, electronically steerable directional antennas can be implemented as patterns of metal on the circuit board. Directivity gains of 10-20 dB at each end are therefore easy to obtain at 60 GHz, which more than compensates for the higher propagation loss. In addition to the increased power efficiency, directional transmission and reception simplifies the transceiver design by significantly reducing the delay spread.
- Due to the smaller wavelength, the capability to diffract around obstacles is far less for 60 GHz than for 5 GHz. For example, if directional antennas are used at either end, a human in the LOS path between the transmitter and receiver can attenuate the signal by 20-30 dB, effectively resulting in link outage.

• Due to the high attenuation of mm waves by walls and obstacles, the range of interest for an indoor mm wave network is of the order of 10 meters, sufficient for an in-room WPAN. The transmit power required for such ranges is small enough to be realizable with ICs using low-cost CMOS and SiGe semiconductor processes.
• Due to the high bandwidth of operation, 60 GHz transceivers must use high sampling rates. Since high-resolution, high-speed analog-to-digital converters are both expensive and power-hungry, it is important to simplify the digital signal processing at the physical layer. Directional transmission and reception facilitates this by reducing the delay spread, and hence the intersymbol interference.

Multihop WPAN with Directional LOS links: Motivated by the preceding considerations, we propose the following architecture for an in-room 60 GHz WPAN. Each node in the network is equipped with an electronically steerable directional antenna, and transmitters and receivers can steer beams towards each other (this implies, for example, that a given node cannot be expected to hear transmissions intended for other nodes). The network employs multihop routing based on directional, LOS links. Each link operates at a fixed nominal data rate (e.g., 2 Gbps) when the LOS path is available. If the LOS path is blocked, we simply route around the link. This design choice is made based on considerations of power efficiency. A link whose LOS path is blocked might still be able to operate at a lower rate, exploiting reflections that reach the receiver. However, if the received power is, say, 10 dB lower, then we must reduce the bit rate by a factor of 10 in order to maintain the same reliability, when operating in power-efficient mode. In contrast, replacing the blocked path by 2 links in a multihop architecture only reduces the throughput by a factor of 2. Our central thesis is that, assuming that there are enough spatially dispersed nodes (including relays, if necessary), multihop networking with directional LOS links provides the best of both worlds: high power efficiency and robust connectivity in the face of stationary and moving obstacles typical of living room and office environments.

Connectivity Model: We use a diffraction model based on the Huygens' principle to determine, for a given configuration of obstacles, whether a given link is blocked or not. This provides a simple deterministic model to track the time evolution of network connectivity for a given set of stationary and mobile obstacles (the geometry of the latter models a human).

Directional MAC: We specify a MAC for directive links for the specific scenario of an in-room WPAN of several wireless terminals (WTs) controlled by a single access point (AP). The ideas can be generalized quite easily to peer-to-peer topologies. The set-up phase involves sectorized transmission of a beacon by the AP, in order to discover the WTs in each of its sectors. WTs hearing the beacon train their antenna arrays to focus on the signal received from the AP, and transmit back to the AP along the same direction, using reciprocity. Contention is resolved using Aloha-like mechanisms in the set-up phase. The AP also instructs each WT to discover its own topology (this knowledge is used for multihop routing when needed). Once the set-up phase is complete, the protocol allows contention-free communication between the AP and the WTs, while setting aside some bandwidth for procuring topology updates. A link blockage is discovered by the AP by a lack of response from a WT when the AP polls it; when this happens, the AP sets up an alternate route based on the topology information it knows. Due to the slow time scale of human movements (which are typically the cause of network topology changes) relative to the topology updates enabled by the protocol, we find that the alternate routes computed by the AP are invariably functional. We provide estimates of the overhead incurred by the proposed MAC protocol, and verify the efficacy of its mechanism for routing around blocked links using simulations of the diffraction-based connectivity model. We conclude that, while outage rates for a given link can be quite high (e.g., 20%), multihop networking effectively removes outages in connectivity between the AP and the WTs.

Related Work: Our work is motivated by recent advances in mm wave circuit design [5], [4] that indicate low-cost IC realizations of mm wave nodes should be available in the near future. This promised cost reduction, together with the fact that directional antennas can be realized in small form factors, motivates our network architecture featuring directional links and relays (if needed). Millimeter wave propagation measurement and modeling have received extensive attention over the past decade. Measurement campaigns in indoor environments include [7], [8], [9], [10], [11], [12]. For typical indoor environments with omnidirectional antennas, specular reflections from surfaces are dominant contributors to the received signal power as compared to diffraction or scattering [13], [14], [15], [11]. Many deterministic and statistical mm wave propagation models have been proposed based on channel measurement studies [13], [12], [16]. However, most of these focus on omnidirectional transmission (and possibly directional reception). The effect of human movements on radio propagation in different microwave bands is investigated in [15] using a 3-dimensional image based ray tracing technique that considers reflection and diffraction effects from human bodies. The benefits of base station diversity in reducing link blockage for omnidirectional transmission is analyzed in [17] for a simple model of an office environment. The reduction of multipath for directional links is well known [10], [18], [17], as is the susceptibility of directional mm wave links to blockage due to their weak diffraction characteristics [10], [1].

To the best of our knowledge, there is no significant prior published work on the design of mm wave WPANs with directional links.

Paper Outline: The rest of the paper is organized as follows. We describe our physical layer model in Section II. Section III presents our multihop relaying based directional MAC framework. In Section IV, we present an approximate analysis to understand the data rate capacity and other characteristics of our MAC scheme. We describe our evaluation methodology and discuss our results in Section V. We conclude the paper with a discussion of our findings and outline the future work in Section VI.

II. Physical Layer Model

We first give an example link budget for a LOS 60 GHz link, to give a feel for the feasibility of WPANs with directional LOS links. However, we then abstract away from detailed design choices to focus on the key bottleneck for mm wave communication: blockage by obstacles.

A. Sample Link Budget

We first present simple calculations indicating the feasibility of a plug-and-play WPAN with antenna directivities of 10 dB. The directivity of an antenna is the ratio of the maximum power density (watts/m^2) to its average value over a sphere. The directivity of an antenna can be approximated as [19]:

$$D = \frac{40000}{\theta^o_{HP}\phi^o_{HP}}$$

where θ^o_{HP} and ϕ^o_{HP} are the horizontal and vertical beamwidths, respectively, of the antenna. For a WPAN application, we might design an antenna element to have a horizontal beamwidth of 120^o and a vertical beamwidth of 60^o, which allows a rough placement of nodes in order to ensure LOS to one or two neighbors. The directivity for such an element, which can be realized as a pattern of metal on circuit board, is 5.55 (or 7.4 dB). If we put four such elements to form a steerable antenna array, we can get a directivity of 22 (or 13.4 dB).

Now, assuming an antenna directivity of 10 dB at each end, we do a link budget for a QPSK system operating at 2 Gbps. For a receiver noise figure of 6 dB, bit error rate of 10^{-9}, excess bandwidth of 33%, and assuming free space propagation, we obtain that the required transmit power for a nominal range of 10 meters is 36 mW, including a 10 dB link margin. When split between four antenna elements, this transmit power corresponds to 9 mW of power per antenna element. RF front ends for realizing these power levels are realizable with CMOS or SiGe processes, indicating the feasibility of low-cost, high-volume production of the kinds of WPAN nodes on which our architecture is based.

B. Link Outage: A Worst-Case Abstraction

We use a simple geometric model to estimate diffraction-based losses along the LOS path between two nodes, taking into account the WT and AP placements, locations and dimensions of obstacles, and room dimensions. We do not consider the contribution from the reflected signals while evaluating the received signal power. This is because our goal is to show that robust connectivity can be obtained using a multihop architecture, even in a worst-case scenario when only energy from the LOS components is being used. Furthermore, narrow beam directional antennas along the LOS direction substantially reduce the contribution of reflected multipath components [18], [10], [15], [17].

We make the following simplifying assumptions in modeling obstacles:
1) We assume that the attenuation due to an obstacle in the LOS path is so high that the energy of the signal propagating through the obstacle is negligible. In other words, we only consider obstacles that can cause a significant attenuation to a signal propagating through them. For mm waves, most of the common obstructions in indoor environments, such as human beings, thick walls and furniture, fall in this category. Thus, the link gain is only due to diffraction around the obstacle.
2) The human body is approximated as a perfect conducting cylinder, whose projection perpendicular to the plane of propagation is considered for diffraction calculations. Other obstacles are approximated in a similar manner.
These assumptions help to significantly reduce complexity, while preserving the essence of the model, which is to capture the fragility of mm wave links in the face of obstacles.

Worst-Case Outage Criterion: We employ the following criterion for link outage: if the diffraction loss due to obstacles exceeds 10 dB for a link, then it is considered to be in outage. This model is pessimistic because link budgets are determined based on a maximum range of operation (10 meters in our case, for in-room operation). Thus, links over shorter ranges may have enough link margin to "burn through" obstacles. For example, a 3 meter range link may be able to sustain a 10 dB diffraction-related loss, since its free-space propagation loss is 10 dB smaller than that at the budgeted distance of 10 meters. By abstracting away the dependence of connectivity on range, we obtain a worst-case network connectivity model that serves to stress-test our proposed multihop architecture.

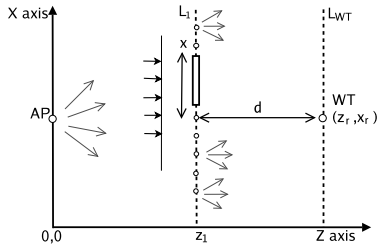

Fig. 1. Diffraction for a single obstacle.

C. Diffraction due to Obstacles

Diffraction of electromagnetic waves can be explained by a fundamental principle from physical optics: the Huygens' principle which states that "*each point on a primary wavefront can be considered to be a new source of a secondary spherical wave and that a secondary wavefront can be constructed as the envelope of these secondary spherical waves*" [20]. Reference [20] provides a detailed analysis of the phenomenon of diffraction on the basis of this principle and also the geometrical theory of diffraction.

To evaluate the effect of obstacles in terms of power loss, we define diffraction loss as

$$g_{diff} = \frac{E}{E_0}, \tag{1}$$

where E is the electric field at the point of observation with diffraction effects and E_0 is the electric field at the same point in an unobstructed environment, given by $E_0 = \frac{A}{d}e^{-j\beta d}$, where A is a constant, and $\beta = \frac{2\pi}{\lambda}$ is the phase constant for

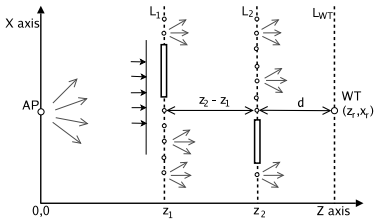

Fig. 2. Multiple obstacles scenario.

wavelength λ. Obviously, for an unobstructed case, $g_{diff} = 1$. In our case, the AP is considered as the source and the WTs are the observation points. The diffraction loss in dB is given by $L_{dB} = -10log_{10}|g_{diff}|^2$.

The electric field E at the WTs can be calculated using the diffraction analysis based on the Huygens' principle. To illustrate this calculation for single and multiple obstacles between the AP and the WTs, we consider a simple example scenario shown in Fig. 1, which illustrates a planar electromagnetic wave obstructed by a conducting strip. The relative distances and the axes are marked in the figure.

By applying the Huygens' principle, the electric field at point (z_r, x_r) is obtained by summing the electric fields due to point sources on line L_1 passing through the obstacle and parallel to the X axis, and is given by

$$E(x_r) = E_0 \int_{-\infty}^{\infty} T(x) e^{-j\beta \frac{(x-x_r)^2}{2d}} dx, \qquad (2)$$

where function $T(x)$ is defined as

$$T(x) = \begin{cases} 1 & \text{for x} \in \{obstacle\}\prime \\ 0 & \text{for x} \in \{obstacle\}, \end{cases}$$

and $d = z_r - z_1$, the separation between the obstacle's z coordinate and the WT's z coordinate. Therefore, the diffraction loss value at the receiver WT is given by

$$g_{diff}(x_r) = \frac{E(x_r)}{E_0(x_r)} = \int_{-\infty}^{\infty} T(x) e^{-j\beta \frac{(x-x_r)^2}{2d}} dx. \qquad (3)$$

This expression for diffraction loss can be viewed as a convolution of $T(x)$ with $e^{-j\beta \frac{x^2}{2d}}$. From *fourier transform* properties, we have

$$\mathcal{F}\{g_{diff}(x_r)\} = \mathcal{F}\{T * e^{-j\beta \frac{x^2}{2d}}(x_r)\} = \mathcal{F}\{T(x)\}\mathcal{F}\{e^{-j\beta \frac{(x)^2}{2d}}\}. \qquad (4)$$

This formulation lends itself to simple computations based on the *Fast Fourier Transform* (FFT) and *Inverse Fast Fourier Transform* (IFFT) techniques and also simplifies the analysis for the multiple obstacle case. We exploit this property to formulate a recursive algorithm to calculate the diffraction loss in case of multiple obstacles between the AP and the WT.

D. Multiple Obstacles

Consider the scenario illustrated in Fig. 2 where there are two obstacles between the AP and the WT. Our goal is to evaluate the diffraction loss because of these obstacles.

We first consider an observation point (z_2, x_2) on the line L_2 that is parallel to the X axis and passes through the second obstacle. From our analysis for the single obstacle case, we find that the diffraction loss at (z_2, x_2) is $g_{diff}(x_2)$. Now all points on line L_2 form new secondary wave sources for further diffraction loss because of the second obstacle on line L_2 (Huygens' principle). Thus, the total diffraction loss at the WT can be evaluated as

$$g_{diff}(x_r) = \int_{-\infty}^{\infty} g_{diff}(x_2) T(x_2) e^{-j\beta \frac{(x_r - x_2)^2}{2(z_r - z_2)}} dx_2, \qquad (5)$$

where (z_r, x_r) is the location of the obstacle. Equation 5 can be viewed as the convolution of two functions $f_{diff}(x)$ and $e^{-j\beta \frac{x^2}{2(z_r - z_2)}}$, where $f_{diff}(x) = g_{diff}(x)T(x)$. Therefore,

$$\mathcal{F}\{g_{diff}(x_r)\} = \mathcal{F}\{f_{diff}(x)\}\mathcal{F}\{e^{-j\beta \frac{(x)^2}{2(z_r - z_2)}}\}, \qquad (6)$$

which can be computed using FFT and IFFT algorithms. This analysis can be extended to the m obstacle case in the following manner:

$$\begin{aligned} \mathcal{F}\{g^m_{diff}(x_r)\} &= \mathcal{F}\{f_{diff}(x)\}\mathcal{F}\{e^{-j\beta \frac{(x)^2}{2(z_r - z_m)}}\} \\ &= \mathcal{F}\{g^{(m-1)}_{diff}(x) T^m(x)\}\mathcal{F}\{e^{-j\beta \frac{(x)^2}{2(z_r - z_m)}}\}, \end{aligned}$$

where $g^{(m-1)}_{diff}(x)$ is the diffraction loss due to the $(m-1)^{th}$ obstacle, evaluated at (z_m, x). We can use this relation recursively starting from the nearest obstacle to the AP and moving towards the next obstacles and then use the IFFT to obtain the final diffraction loss at the WT (z_r, x_r).

III. Directional MAC Design

The key idea behind our multihop relay directional MAC framework is to utilize a mix of the conventional AP-based single wireless hop MAC architecture for primary connectivity and resort to the multihop ad hoc mode with intermediate nodes acting as relays (though still controlled by the AP) to prevent drastic reduction of data rates or link outage when the LOS component to a WT is obstructed. Because of directional transmissions at all nodes, the conventional carrier sensing solutions are not suited for mm wave WPANs.

The indoor environment is split into different coverage sectors. The AP transmits directionally to cover one sector per transmission. Medium access inside each sector is arbitrated through a IEEE 802.11 PCF contention-free polling-based scheme where the AP sequentially polls each node for data transfer. The placement of the AP and the WTs is assumed to be reasonably intelligent such that none of the nodes are initially placed in such a manner that they are totally isolated from the network. The AP sequentially transmits in each of its sectors and it can alter the antenna dwell time in each sector based on control and data transfer requirements. Each WT registers with the AP in response to the strongest beacon it receives (LOS component) from the AP, and trains its antenna array in the direction of the LOS component to maximize the received signal power. In the following sections, we describe our directional MAC framework in detail.

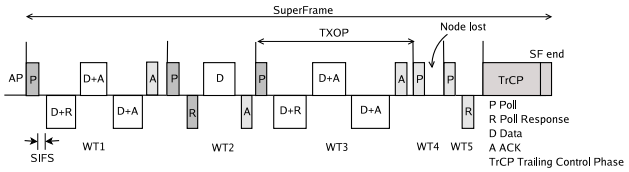

Fig. 3. An example MAC message sequence over a superframe.

A. Discovery Algorithm

During the network initialization phase, the AP sends a *Hello message* and waits for response from WTs in each sector. On receiving a Hello message, the WTs adjust their antenna beams to maximize the received power from the AP and respond with the Hello Response message. The WTs in each sector employ a Slotted Aloha [21] contention scheme, with probabilities of transmission dictated by the AP. After performing this discovery process in each sector, the AP iteratively designates each WT among the registered nodes to perform the same discovery procedure. This process continues until all the WTs in the network have finished the discovery procedure and have created their own network topology maps (i.e., each WT is aware of the identities of the other WTs and the appropriate antenna array configurations/directions required to reach them). Every WT in the network sends its network topology map to the AP after it completes its network discovery process. This information helps the AP deduce the link connectivity status of the whole network, which is useful in determination of a relay WT when a node is lost. The topology maps created during the initialization phase are therefore useful for lost node discovery and data transmission procedures, as described in the next sections.

B. Normal Mode of Operation

The AP does a poll similar to the IEEE 802.11 PCF poll in each sector to check connectivity to each WT in that sector and to check whether a WT has data to transmit. Each WT must respond within a fixed interval, i.e., Poll Inter Frame Space (PIFS), with a data packet if it has data to transmit or with a *connection live* poll response message even if it does not have data to transmit. This PCF-based procedure is necessary because conventional carrier sensing medium contention schemes do not work well with directional antennas. The polling scheme also helps the AP to track LOS connectivity to all the registered WTs. The dwell times in each sector depend on the data transmission requirements of the nodes residing in that sector. The AP to WT data transmission mechanism follows a weighted round robin scheduling approach.

The WT can continue to receive data packets from the AP or send data packets to the AP until a maximum allowed time duration called the *transmission opportunity* (TXOP) duration. Thus, data transmission in both directions can be bursty due to the sequential transmission of multiple packets in response to the poll message, up to the TXOP duration. This allows the WTs to better utilize the available LOS connectivity and also minimizes the control overhead associated with data packet transmissions. If the AP sends a data packet to a WT, the WT acknowledges the successful packet reception by piggybacking an ACK message on the next data packet that it has for the AP. Otherwise, if the WT does not have any data to send to the AP, it just sends an ACK message.

C. Trailing Control Phase

The trailing control phase is used by the AP to allow new nodes to register and to perform a network discovery procedure while the network is operational. During the trailing control phase, the AP can also verify its own topology map or designate registered WTs to verify their network topology map by sequentially sending Hello messages to each WT. This phase helps the AP and WTs to track changes in the network topology map due to link connectivity losses from human beings, other obstacles, occasional changes in the room configuration or movements of the WTs. It also allows the AP to take care of other control requirements such as *superframe* end signaling, where a superframe is defined as the time taken by the AP to poll all the registered WTs in the network. The trailing control phase is limited to a maximum duration, which is higher than the average successful discovery phase time of a node. Because the regular network topology verification procedure of the trailing control phase occurs at a rate much faster than the dynamics of the indoor environments (human movements or change in room setup), the AP is aware of LOS connectivity of all the WTs and it can choose from candidate relay nodes for a lost WT based on the topology verification/discovery reports sent back by the WTs.

The maximum superframe duration is limited by the number of WTs in the network, the TXOP duration, and the trailing control phase duration. The AP signals the end of a superframe after the trailing control phase functions are finished. Fig. 3 illustrates an example of data transmission and control message sequence over a superframe for a network comprised of an AP and five WTs.

D. Lost Node Discovery

If the AP does not receive a poll response from a registered WT within the PIFS interval, it considers the WT to be *lost* and intelligently chooses a WT among the *live* WTs in the neighboring sectors (with expected LOS connectivity to the lost WT as determined from the regular topology verification reports from the WTs) to act as relay to the lost node. It commands the chosen relay WT to discover (i.e., check connectivity status with) the lost WT and report back within a stipulated time. The designated relay WT refers to its network topology map information to steer its antenna beam to the lost WT, and sends a Hello message to the lost WT. If the lost WT is able to receive this message, it adjusts its antenna beam towards the designated relay WT and responds with a Hello Response message. Upon receiving a reply from the lost WT, the chosen relay WT reports to the AP the quality of the link (i.e., the received signal strength) between itself and the lost WT. Otherwise, after waiting for a PIFS interval, it informs the AP of discovery failure. Depending on the response from

the designated relay WT, the AP decides whether to choose another WT in the poll sequence to repeat the lost node discovery procedure or to use the current chosen WT as a relay for future data transfers until the LOS connectivity to the lost WT is restored. The relay WT acts as a *pseudo AP* to the lost WT. Upon a successful lost WT discovery, the AP adds the required data transfer time for the lost WT to the relay WT's sector dwell time. Once the obstruction is removed and the lost WT starts receiving direct transmissions from the AP, it responds to the AP's poll message. The AP switches back to the normal mode of operation after informing the relay WT to return to its previous state. The dwell times for the directional transmissions in different sectors are adjusted accordingly.

IV. Achievable Rates

In this section, we estimate the aggregate data transfer capacity of our multihop MAC framework. We first find the aggregate throughput for the case when no WT is blocked and packet transmissions to the WTs from the AP are single hop. Then we calculate the change in throughput for cases when the LOS connectivity to some WTs is lost, and multihop relay is used as an alternative mechanism to maintain connectivity. The goal is that this results in graceful degradation of overall network throughput rather than loss of connectivity to such WTs altogether, which is extremely undesirable. Given the high data rates afforded by 60 GHz transceiver systems, this reduction in the aggregate throughput does not affect the applications unless network is operating at full capacity, which is unlikely to be true in general scenarios. Also, in order to provide the required quality of service (QoS) support to different WPAN applications, maintaining connectivity to all the nodes is essential.

We consider QPSK modulation at 2 Gbps, as in the system described in Section II-A. We assume that 200 symbols are required for synchronization, adding 200ns of synchronization overhead. While this is adequate for the single carrier system we envision, OFDM might incur additional overhead; the framework for our analysis, however, would remain identical. The physical layer control protocol overhead is assumed to be 50ns. Thus, the total PHY overhead for each data transmission is 250ns. We also assume that all the nodes operate at the same data rate. The maximum allowed TXOP duration is assumed to be 50μs. The AP polls each registered WT once per superframe and checks connectivity. The superframe duration is allowed to vary as per the data requirements of WTs, but it is limited to a maximum duration (determined by the TXOP interval, the number of WTs, and the system configuration).

We find the maximum aggregate throughput sustained by the network, assuming backlogged UDP flows from the AP to all the WTs with a packet size of 1000 bytes. This UDP based application model can incorporate the requirements of common WPAN applications including streaming content download for HDTV, real time streaming and wireless data bus. Table I lists our notation and parameter values.

The total time required to transmit a packet is given by

$$T_{pkt} = T_{PHY} + T_{hdr} + T_{payload} = 4.474\mu s. \quad (7)$$

Parameter	Symbol	Value
PHY data rate	R	2 Gbps
PHY overhead	T_{PHY}	250ns
Header overhead (IP+UDP+MAC)	T_{hdr}	56*8/R
Payload Tx time	$T_{payload}$	1000*8/R
Short MAC frame Tx time	T_{ShFr}	$T_{PHY} + 14 * 8/R$
SIFS interval	T_{SIFS}	100ns
ACK Tx time	T_{ACK}	T_{ShFr}
TXOP duration	T_{TXOP}	50μs
Polling overhead	T_{poll}	$2T_{ShFr} + T_{SIFS}$
Maximum Trailing Control period	T_{TrCP}	50μs
Maximum Superframe duration	T_{SF}	2ms
Hello/Hello Response Tx time	T_H/T_{HR}	T_{ShFr}

TABLE I
PARAMETERS

Every successfully received packet from the AP is acknowledged by an ACK message from the WT since the WTs do not have reverse data traffic. Thus, the total number of packets transmitted in one TXOP is given by

$$N_{pkt} = \frac{T_{TXOP} - T_{poll}}{T_{pkt} + T_{SIFS} + T_{ACK}} = 10. \quad (8)$$

In a network consisting of n active WTs fully utilizing their TXOP duration, the total superframe time will be $T_{SF} = n{\cdot}T_{TXOP} + T_{TrCP}$, which for an eight WT network evaluates to 450μs. We note that this duration is still small enough such that the AP and WTs can closely monitor changes in network topology and they can adapt to the dynamics of the indoor environment by using multihop relays. Thus, the aggregate throughput S_{SH} sustained by the network under consideration is given by

$$S_{SH} = \frac{n{\cdot}N_{pkt}{\cdot}P_{size}}{T_{SF}}, \quad (9)$$

which equals 1.4222 Gbps for the eight WT case. If we assume that m out of n nodes in the network are connected through two hop paths, the T_{SF} increases by mT_{TXOP} to facilitate data transfer over multihop paths without any packet loss. The aggregate throughput S_{MHR} in that case will be

$$S_{MHR} = \frac{n{\cdot}N_{pkt}{\cdot}P_{size}}{T_{SF} + m{\cdot}T_{TXOP}}. \quad (10)$$

For an eight WT network with two WTs using relays for data transfer, the aggregate throughput is 1.1636 Gbps. This reduction in aggregate network throughput (as compared with 1.4222 Gbps in full single hop connectivity case) is the cost paid in order to maintain connectivity to all the active WTs in the network and to ensure that even the *lost* WTs do not suffer from packet loss because of blockage of the direct link to the AP. We therefore consider this reduction in the aggregate network throughput as graceful throughput degradation.

A. Initialization and Discovery Phase

We estimate the average time required for the initialization phase started by the AP where each node discovers the network topology map using the discovery algorithm described in Section III. The AP transmits a Hello message in a sector containing the transmit probability to be used by the nodes that

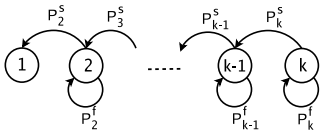

Fig. 4. Markov chain modeling discovery procedure in a sector.

respond in the next slots. We define a slot as the total time elapsed for a successful registration that requires the Hello Response message from the registering WT followed by the corresponding ACK from the AP. A slot duration T_{reg} is given by

$$T_{reg} = T_{HR} + 2 * T_{SIFS} + T_{ACK}. \quad (11)$$

Although the Hello Response message from one WT might not be heard by other WTs in that sector, the AP's ACK following a successful registration or a failed registration attempt (defined by collision of Hello Response messages from different WTs) is heard by all the WTs in the sector. The ACK message also contains the transmission probabilities to be used by the unregistered WTs for their Hello Response transmission attempts over the next slots. This procedure allows the AP to effectively control the Hello Response packet collisions. We note that because there is likely to be few WTs in each sector, the problem of excess collisions is unlikely. For this reason, we assume a fixed transmission probability p for the Hello responses.

Consider a network discovery scenario with n nodes in a sector, with the AP trying to discover the WTs by sending a Hello message and waiting for Hello responses from the WTs. The WTs employ a medium access scheme similar to Slotted Aloha, where each unregistered WT probabilistically transmits a Hello Response message depending on the transmission probability. Our aim is to obtain an estimate of the average time required for all the WTs in the sector to successfully register with the AP. We can model the initialization phase as a Markov chain as shown in Fig. 4, with its states defined as the number of unregistered WTs k in the sector and transition probability P_k^s defined as the probability of successful registration by a WT such that a Hello Response message is transmitted by a WT in a slot and it reaches the AP without colliding with other WTs' Hello Response messages. P_k^f is defined as the probability of registration failure in a slot either because of collision of Hello responses from multiple WTs or because no WT transmits over that slot. Thus,

$$P_k^s = kp(1-p)^{(k-1)}, \text{ and } P_k^f = 1 - P_k^s. \quad (12)$$

The cost associated with each failed or successful transition attempt is one slot. Therefore, the expected cost of transition from state k to state $k-1$ is given by

$$C_{(k \to k-1)} = P_k^s(1 + \sum_{i=1}^{\infty} i(P_k^f)^i) = P_k^s + \frac{P_k^f}{P_k^s}. \quad (13)$$

Thus, the total expected slots required for discovery and registration of all the n nodes in the sector is given by the total expected cost of transition from the initial state of n nodes to final state of only one node in the Markov chain:

$$T_{disc}^{slot} = 1 + \sum_{k=2}^{n} C_{(k \to k-1)}, \quad (14)$$

where an extra slot is added to account for the last node registration.

Consider an example scenario of a network with three sectors, where each sector has four WTs and the probability of a Hello response transmission by WTs over a slot is 0.2. The expected discovery time for the network is obtained as 22 slots or 17.86μs. We note that at these time scales, the processing delay at the AP and the WTs are non-negligible and should be accounted for in order to get the actual delays. Because these factors appear in all our time approximations, they will cause a similar shift in these estimates. Thus, the initial discovery phase duration of 100μs should be sufficient in the network, and the trailing control phase can be used for running the discovery algorithm at a WT.

Parameter	Value
Link loss margin	10 dB
Human height range	(1.5m - 2.1m)
RWP model velocities (min,max)	(0m/s,1m/s)
RWP model pause time	10s
Fixed obstacle height range	(1m - 1.4m)
WT location height range	(0.5m - 1.5m)
AP location heights home/office	2m/2.5m
Simulation time	5min

TABLE II
EVALUATION MODEL PARAMETERS

V. PERFORMANCE EVALUATION

In this section, we describe our evaluation methodology and present performance results for our multihop relay directional MAC scheme in comparison to the conventional single hop AP to WT communication MAC schemes such as the infrastructure mode of the IEEE 802.11 MAC. We call the single hop communication scheme as the baseline MAC.

A. Simulation Model

We have developed a MatLab-based tool to evaluate the performance of our multihop relay MAC scheme by simulating different indoor environments with human beings and other obstacles. This tool is based on our deterministic physical radio propagation model described in Section II which yields link connectivity between different network nodes given the link margin. The inputs to our tool are parameters required to simulate a WPAN in a specified 3-dimensional indoor environment: the room dimensions; the number, position, and dimensions of stationary obstacles such as furniture; the number of human beings; the placement of the AP; and the number and positions of the WTs. We use the Random Waypoint model for human movements in the floor area of rooms. The default configuration parameters related to the test scenarios are listed in Table II.

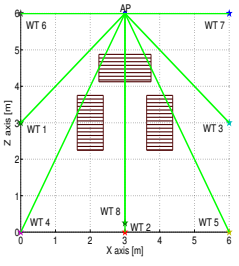

Fig. 5. Living room scenario.

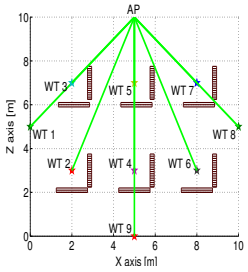

Fig. 6. Office space scenario.

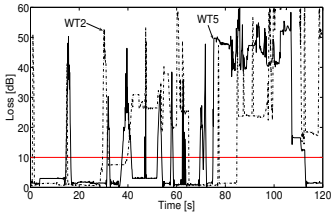

Fig. 7. Living room: AP to WT LOS link loss profile.

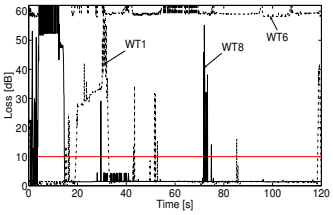

Fig. 8. Office: AP to WT LOS link loss profile.

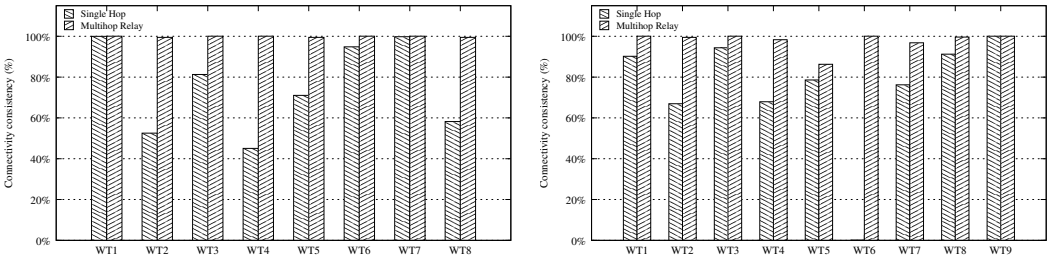

(a) Living room

(b) Office

Fig. 9. Connectivity consistency from the AP to different WTs in single hop baseline and multihop relay MAC.

We evaluate the performance of our directional MAC scheme based on the following metrics. We define *connectivity consistency* as the percentage of time out of the total operation period of the network when a WT is reachable from the AP, either through a direct LOS link or through a multihop path consisting of live direct links. We also evaluate the expected aggregate network throughput and study its variation over time with respect to dynamics of the indoor environments such as obstacle movements.

We note that connectivity consistency is an indirect metric because the need for connectivity arises only if there is data to transmit at either side. However, considering the importance of an LOS link for maintaining direct connectivity (unlike for 2.4 or 5 GHz WLANs), the links can become blocked easily due to obstacles in indoor environments. Thus, this metric characterizes the actual connection state and data transfer capacity of the network. This metric can also be interpreted as an indicator of the maximum aggregate throughput sustained by the network when all the nodes have data to send.

We evaluate the performance of our framework for two different indoor environments that model typical scenarios where 60 GHz WPANs are expected to be deployed: a living room and an office space (see Figs. 5 and 6). The living room scenario has a WPAN formed by an HDTV, surround sound system with speakers at room corners, and a desktop/printer; and has eight human beings, i.e., during a gathering at home. The office space scenario has desktops and printers forming a WPAN, with fifteen human beings. The room and obstacle dimensions and node placements have been chosen as representative of real world scenarios in which a large number of people can cause a high blockage probability for individual links. Note that WT1 in the home scenario and WT9 in the office scenario are placed higher than the other WTs (2.5m, compared to 1.2m on average for the other WTs) such that they have a high probability of a clear LOS connectivity to most of the WTs and the AP. Hence they can act as effective relays in case the direct LOS connectivity from the AP to a WT is blocked.

Figs. 7 and 8 plot the variation of link loss for some specific WT links as a function of time for home and office environments over a sample period of 120 seconds. We observe that there are heavy link losses because of the large number of human beings and their random movements and stationary furniture obstacles in both the environments. These obstacles result in intermittent connectivity to the affected WT if the underlying MAC completely relies on direct single hop connectivity of the AP to WTs. These loss results demonstrate that networks with the baseline MAC scheme will not be able to provide the required QoS or data rate guarantees to different WPAN applications, which are essential requirements for any practical WPAN solution.

Fig. 9 compares the connectivity consistency between the baseline MAC scheme and our directional multihop relay MAC scheme for WTs in the two environments. We observe that, on average, connectivity consistency in the baseline case is significantly lower than the multihop relay MAC scheme, which is able to maintain almost 100% network connectivity. Note that the availability of alternate routes in a multihop architecture can be easily ensured by appropriate placement of relay nodes (e.g., high up on walls, or on the ceiling). On the other hand, the poor connectivity consistency of single hop communication makes it unsuitable for WPAN applications with stringent QoS requirements such as video streaming.

Figs. 10 and 11 plot the expected aggregate network throughput variation for our multihop relay MAC scheme as a

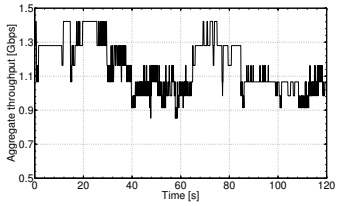

Fig. 10. Living room: aggregate network throughput.

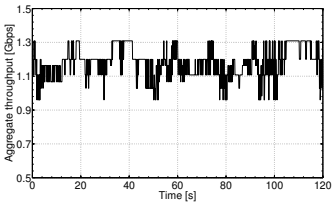

Fig. 11. Office: aggregate network throughput.

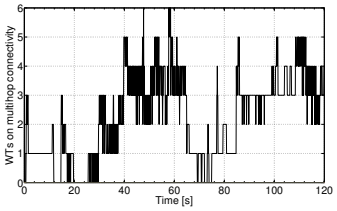

Fig. 12. Living room: number of WTs connected via relays.

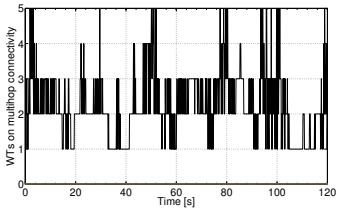

Fig. 13. Office: number of WTs connected via relays.

function of time. We observe that the aggregate throughput remains fairly consistent, even in presence of moving and stationary obstacles. Since we have already seen the poor connectivity consistency of a single hop MAC, we do not plot aggregate throughput for the latter. Figs. 12 and 13 depict the number of WTs connected via multihop paths at different sampling instances of the simulation. We infer that at any time instant, there are a significant number of WTs that are using a multihop relay, which indicates the importance of multihop paths in maintaining continuous network connectivity.

VI. Conclusions

Our results illustrate the critical role of cross-layer design in exploiting the large unlicensed bandwidth available in the 60 GHz band. The simple diffraction-based connectivity model is an effective tool for cross-layer design: it yields results that conform to our intuition that directional LOS mm wave links experience relatively high levels of outage due to stationary and moving obstacles. Despite this fragility of individual links, we show that the proposed multihop MAC architecture is successful in providing robust connectivity in typical "Superbowl Party" and office settings. Thus, unlike infrastructure mode operation in 2.4 GHz and 5 GHz WLANs, where WTs communicate with APs over a single hop, we believe that multihop communication, possibly with nodes explicitly designated as relays, must play a fundamental role in 60 GHz WPANs. Our future work therefore focuses on refining the proposed multihop design based on more detailed modeling and simulation. At the physical layer, detailed evaluation of packetized systems for specific modulation formats (e.g., a comparison of single carrier modulation and OFDM under more detailed propagation models for directional links) is necessary. At the application layer, it is of interest to evaluate MAC performance in more detail using traffic models aimed specifically at some of the entertainment applications driving the interest in high-speed WPANs, such as streaming compressed and uncompressed HDTV, as well as large file transfers (e.g., modeling digital camera or movie content).

References

[1] P. F. M. Smulders, "Exploiting the 60 GHz Band for Local Wireless Multimedia Access: Prospects and Future Directions," *IEEE Commun. Mag.*, vol. 40, no. 1, pp. 140–147, Jan. 2002.

[2] F. Giannetti, M. Luise, and R. Reggiannini, "Mobile and Personal Communications in the 60 GHz Band: A Survey," *Wireless Pers. Commun.*, vol. 10, no. 2, pp. 207–243, Jul. 1999.

[3] (2004, March) IEEE 802.15 WPAN Millimeter Wave Alternative PHY Task Group 3c (TG3c). [Online]. Available: http://www.ieee802.org/15/pub/TG3c.html

[4] (2006) IBMs 60-GHz Page. [Online]. Available: http://domino.research.ibm.com/comm/research_projects.nsf/pages/mmwave.%sixtygig.html

[5] (2006) 60 GHz CMOS Radio Design at Berkeley Wireless Reaearch Center. [Online]. Available: http://bwrc.eecs.berkeley.edu/Research/RF/ogre_project/

[6] (2006) WIGWAM - Wireless Gigabit with Advanced Multimedia Support. [Online]. Available: http://www.wigwam-project.de/

[7] H. Xu, V. Kukshya, and T. S. Rappaport, "Spatial and Temporal Characteristics of 60 GHz Indoor Channels," *IEEE J. Sel. Areas Commun.*, vol. 20, no. 3, pp. 620–630, Apr. 2002.

[8] N. Moraitis and P. Constantinou, "Indoor Channel Measurements and Characterization at 60 GHz for Wireless Local Area Network Applications," *IEEE Trans. Antennas Propag.*, vol. 52, no. 12, pp. 3180–3189, Dec. 2004.

[9] P. F. M. Smulders, "Broadband Wireless LANs: A Feasibility Study," Ph.D. dissertation, Eindhoven University of Technology, The Netherlands, 1995.

[10] T. Manabe, K. Sato, H. Masuzawa, K. Taira, T. Ihara, Y. Kasashima, and K. Yamaki, "Effects of Antenna Directivity and Polarization on Indoor Multipath Propagation Characteristics at 60 GHz," *IEEE J. Sel. Areas Commun.*, vol. 14, no. 3, pp. 441–448, Apr. 1996.

[11] H. Yang, M. Herben, and P. Smulders, "Impact of Antenna Pattern and Reflective Environment on 60 GHz Indoor Radio Channel Characteristics," *IEEE Antennas Wireless Propagat. Lett.*, vol. 4, pp. 300–303, Jun. 2005.

[12] J. Kunisch, E. Zollinger, J. Pamp, and A. Winkelmann, "MEDIAN 60GHz Wideband Indoor Radio Channel Measurements and Model," in *Proc. 50th Vehicular Technology Conference, VTC'99*, Amsterdam, The Netherlands, Sep. 1999.

[13] P. F. M. Smulders, "Deterministic Modelling of Indoor Radio Propagation at 4060 GHz," *Wireless Pers. Commun.*, vol. 1, no. 2, pp. 127–135, Jun. 1994.

[14] F. Villanese, N. E. Evans, and W. G. Scanlon, "Pedestrian-Induced Fading for Indoor Channels at 2.45, 5.7 and 62GHz," in *Proc. 52th Vehicular Technology Conference, VTC'00*, Boston, MA, Sep. 2000.

[15] M. Williamson, G. E. Athanasiadou, and A. R. Nix, "Investigating the Effects of Antenna Directivity on Wireless Indoor Communication at 60GHz," in *Proc. IEEE PIMRC'97*, Helsinki, Finland, Sep. 1997.

[16] R. Janaswamy, "An Indoor Pathloss Model at 60 GHz Based on Transport Theory," *IEEE Antennas Wireless Propagat. Lett.*, vol. 5, pp. 58–60, 2006.

[17] K. Sato and T. Manabe, "Estimation of Propagation-Path Visibility for Indoor Wireless LAN Systems under Shadowing Condition by Human Bodies," in *Proc. 48th Vehicular Technology Conference, VTC'98*, Ottawa, Canada, May 1998.

[18] T. Manabe, K. Sato, H. Masuzawa, K. Taira, T. Ihara, Y. Kasashima, and K. Yamaki, "Polarization Dependence of Multipath Propagation and High-speed Transmission Characteristics of Indoor Millimeter-Wave Channel at 60 GHz," *IEEE Trans. Veh. Technol.*, vol. 44, no. 2, pp. 268–274, May 1995.

[19] J. D. Kraus, *Antennas for all Applications.* New York: McGraw-Hill, Inc., 2002.

[20] ——, *Electromagnetics*. New York: McGraw-Hill, Inc., 1991.

[21] N. Abramson, "The Throughput of Packet Broadcasting Channels," *IEEE Trans. Commun.*, vol. 25, no. 1, pp. 117–128, Jan. 1977.